

Grain size control of lead-free $\text{Li}_{0.06}(\text{Na}_{0.5}\text{K}_{0.5})_{0.94}\text{NbO}_3$ piezoelectric ceramics by Ba and Ti doping

Ken-ichi Kakimoto*, Kiyotaka Ando, Hitoshi Ohsato

*Department of Materials Science and Engineering, Graduate School of Engineering, Nagoya Institute of Technology,
Gokiso-cho, Showa-ku, Nagoya 466-8555, Japan*

Available online 25 August 2009

Abstract

In this study, Ba- and Ti-doped $\text{Li}_{0.06}(\text{Na}_{0.5}\text{K}_{0.5})_{0.94}\text{NbO}_3$ $[(1-x)\text{Li}_{0.06}(\text{Na}_{0.5}\text{K}_{0.5})_{0.94}\text{NbO}_3-x\text{BaTiO}_3$ ($x=0-0.07$)] ceramics were prepared by using conventional solid state reaction method, and the microstructure and electric properties of these samples were investigated. The grain size distribution of non-doped $\text{Li}_{0.06}(\text{Na}_{0.5}\text{K}_{0.5})_{0.94}\text{NbO}_3$ ceramics was relatively wide. The microstructure was composed of grains ranging 1.1–5.0 μm in size. However, with increasing Ba and Ti content, the grain size distribution became narrow and the average grain size decreased from 2.0 to 0.9 μm in size. In particular, the microstructure of $x=0.07$ sample was composed of grains ranging 0.5–2.2 μm in size. As a result, the frequency dispersion of dielectric constant for the $(1-x)\text{Li}_{0.06}(\text{Na}_{0.5}\text{K}_{0.5})_{0.94}\text{NbO}_3-x\text{BaTiO}_3$ ($x=0-0.07$) ceramics was reduced and the mechanical quality factor Q_m was enhanced with increasing Ba and Ti content.

© 2009 Elsevier Ltd. All rights reserved.

Keywords: Dielectric properties; Ferroelectric properties; Grain size; Lead-free; Piezoelectric properties

1. Introduction

Alkaline niobate compounds have been intensively studied to find potential candidates for lead-free materials because of their excellent piezoelectric properties. In particular $(\text{Na}_{0.5}\text{K}_{0.5})\text{NbO}_3$ -based ceramics were reported to have good piezoelectric properties and high Curie temperature.^{1–14} However, piezoelectric ceramics generally require not only an improvement in piezoelectric properties but also uniform fine-grained microstructure, because they require good mechanical strength to be applied in devices that generate mechanical force and strain.⁶ Therefore, an improvement in the microstructure of $(\text{Na}_{0.5}\text{K}_{0.5})\text{NbO}_3$ -based piezoelectric ceramics was reported by the use of novel sintering aids such as $\text{K}_{5.4}\text{Cu}_{1.3}\text{Ta}_{10}\text{O}_{29}$,^{5,6} CuO ,^{7,8} and ZnO ,^{9,10} or the use of element substitutions such as BaTiO_3 ,¹¹ SrTiO_3 ,¹² and CaTiO_3 .¹³

On the other hand, we reported that $\text{Li}_x(\text{Na}_{0.5}\text{K}_{0.5})_{1-x}\text{NbO}_3$ (LNKN) ceramics were a particularly promising candidate material among the $(\text{Na}_{0.5}\text{K}_{0.5})\text{NbO}_3$ -based ceramics, since LNKN ceramics with $x=0.06$, $\text{Li}_{0.06}(\text{Na}_{0.5}\text{K}_{0.5})_{0.94}\text{NbO}_3$, show the excellent piezoelectric properties; $d_{33}=235$ pC/N, $k_p=0.42$

and $k_t=0.48$ at room temperature.¹ However, the investigation of the microstructure has not been conducted on $\text{Li}_{0.06}(\text{Na}_{0.5}\text{K}_{0.5})_{0.94}\text{NbO}_3$ system. In this study, therefore, Ba- and Ti-doped $\text{Li}_{0.06}(\text{Na}_{0.5}\text{K}_{0.5})_{0.94}\text{NbO}_3$ ceramics were synthesized by using conventional solid state reaction and the microstructure and electric properties of these ceramics were investigated.

2. Experimental

High purity Li_2CO_3 (99.0%), Na_2CO_3 (99.9%), K_2CO_3 (99.9%), Nb_2O_5 (99.9%), BaCO_3 (98.74%) and TiO_2 (99.97%) powders were used as the starting materials. These powders were weighed according to the formula of $(1-x)\text{Li}_{0.06}(\text{Na}_{0.5}\text{K}_{0.5})_{0.94}\text{NbO}_3-x\text{BaTiO}_3$, where x is varied from 0 to 0.07. The weighed powders were mixed and crushed by planetary ball-milling with zirconia balls for 1 h in acetone medium. The dried mixture was calcined at 850 °C for 10 h, followed by grinding again with planetary ball-milling to produce a fine powder. The granulated powders using polyvinyl alcohol (PVA) as a binder were sieved through a 150-mesh screen and pressed uniaxially into disks of 12 mm in diameter. The disks were cold-isostatic-pressed under 200 MPa, and then sintered in air at selected temperatures of 1082 °C ($x=0$),

* Corresponding author. Tel.: +81 52 735 7734; fax: +81 52 735 7734.
E-mail address: kakimoto.kenichi@nitech.ac.jp (K.-i. Kakimoto).

1090 °C ($x=0.01$), 1105 °C ($x=0.03$), 1120 °C ($x=0.05$) and 1135 °C. The calcination and sintering processes were carried out by using a partially sealed crucible containing a powder bed made of $\text{Li}_{0.06}(\text{Na}_{0.5}\text{K}_{0.5})_{0.94}\text{NbO}_3$ powder to provide a closed atmosphere.

The density of sintered ceramics was measured by the Archimedes method. The melting point of sintered ceramics was measured by a thermogravimetry differential thermal analysis instrument (TG–DTA, DTG-60H Shimadzu). The crystalline phase at room temperature was verified by X-ray powder diffraction (XRPD) analysis using a Philips X-pert diffractometer with $\text{Cu K}\alpha$ radiation. The microstructure of the polished samples was observed by scanning electron microscopy (SEM).

Specimens for electrical characterization were prepared from polished samples by firing on a silver electrode. The dielectric constant was measured using a LCR meter (NF ZM2355) in the temperature range from room temperature to 600 °C at frequencies 0.1, 1, 10 and 100 kHz. P – E hysteresis loops were obtained at 1 Hz using an aix-ACCT TF 2000FE-HV ferroelectric test unit with a high-voltage power supply (Trek610D). The electrical

resistivity was measured using a Digital Electrometer (Advantest R8252). Specimens for the piezoelectric measurement were poled in silicone oil at 150 °C by applying a dc electric field of 30 kV/cm for 60 min, and the specimens were cooled to room temperature in the field. The piezoelectric constant d_{33} was measured using quasi-static method by a d_{33} meter (Academia Sinica ZJ-4B). The electromechanical coupling coefficient k_p of the planar mode and the mechanical quality factor Q_m were determined by a resonance and anti-resonance method performed on the basis of IEEE standards using an impedance analyzer (Agilent 4294A).

3. Results and discussion

Fig. 1 shows the X-ray powder diffraction (XRPD) patterns of the $(1-x)\text{Li}_{0.06}(\text{Na}_{0.5}\text{K}_{0.5})_{0.94}\text{NbO}_3-x\text{BaTiO}_3$ ($x=0-0.07$) ceramics. The $x=0$ specimen showed the morphotropic phase boundary (MPB), in which both tetragonal ($P4mm$) and orthorhombic phase ($Bmm2$) coexist, as our group reported.¹ On the other hand, when BaCO_3 and TiO_2 were added to the starting composition, the crystal system of the sintered materials seemed to reduce the c/a ratio of the tetragonal phase (Fig. 1(a)). The position of the (200) and (002) peaks, which are associated with the tetragonality of the crystal, shifted toward a higher angle and a lower angle with increasing the Ba and Ti content,

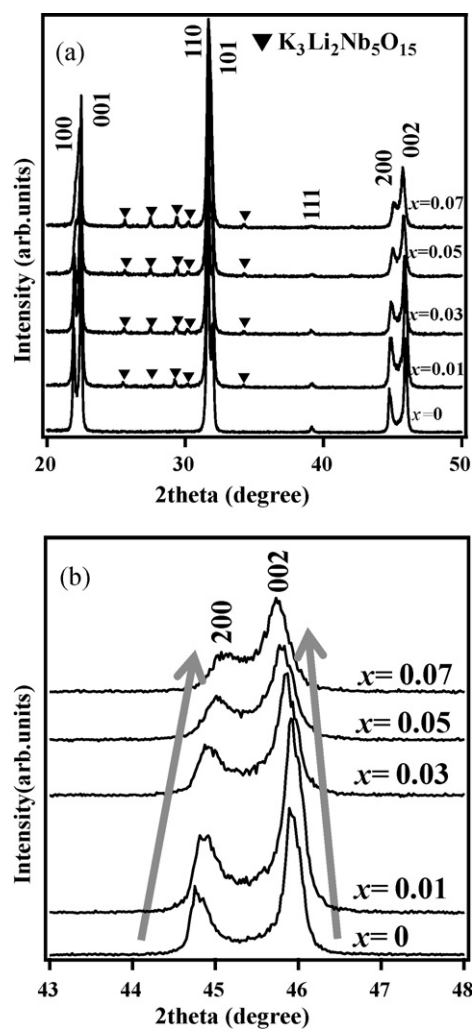


Fig. 1. (a) XRPD patterns of the $(1-x)\text{Li}_{0.06}(\text{Na}_{0.5}\text{K}_{0.5})_{0.94}\text{NbO}_3-x\text{BaTiO}_3$ ($x=0-0.07$) ceramics; (b) magnification of XRPD patterns in the range from 43° to 48°.

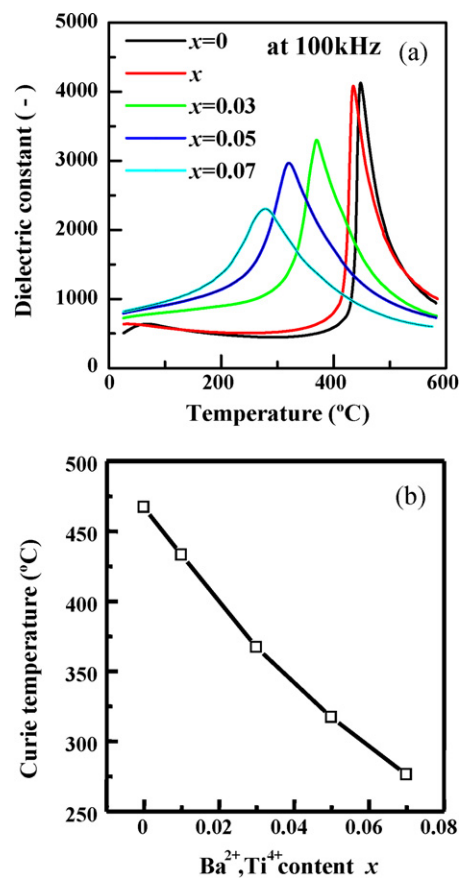


Fig. 2. (a) Temperature dependence of the dielectric constant (ϵ_r) at 100 kHz; (b) Curie temperature variation of the $(1-x)\text{Li}_{0.06}(\text{Na}_{0.5}\text{K}_{0.5})_{0.94}\text{NbO}_3-x\text{BaTiO}_3$ ($x=0-0.07$) ceramics.

respectively (Fig. 1(b)). Therefore, it was expected that Ba and Ti ions could diffuse into the $\text{Li}_{0.06}(\text{Na}_{0.5}\text{K}_{0.5})_{0.94}\text{NbO}_3$ lattice to form a solid solution, although the $\text{K}_3\text{Li}_2\text{Nb}_5\text{O}_{15}$ secondary phase was observed by adding Ba^{2+} and Ti^{4+} ions.

Fig. 2(a) shows the temperature dependence of the dielectric constant (ϵ_r) at 100 kHz of the $(1-x)\text{Li}_{0.06}(\text{Na}_{0.5}\text{K}_{0.5})_{0.94}\text{NbO}_3-x\text{BaTiO}_3$ ($x=0-0.07$) ceramics. For the $x=0$ specimen, two peaks were observed at 447 and 60 °C corresponding to phase transitions from cubic to tetragonal (Curie temperature, T_c) and tetragonal to orthorhombic symmetry, respectively. The phase transition temperature from tetragonal to orthorhombic symmetry decreased with increasing x to be lower than room temperature at $x \geq 0.01$, indicating that its crystal system became tetragonal structure at room temperature in agreement with the XRPD results. With increasing Ba and Ti content x furthermore, the ϵ_r peak at T_c was broadened, indicating the diffuse phase transition due to both A-site and B-site cation mixtures in perovskite structure ABO_3 . This result was similar to the reported dielectric behavior in $(1-x)(\text{Na}_{0.5}\text{K}_{0.5})\text{NbO}_3-x\text{BaTiO}_3$,² $(1-x)(\text{Na}_{0.5}\text{K}_{0.5})\text{NbO}_3-x\text{SrTiO}_3$ ³ and $(1-x)(\text{Na}_{0.5}\text{K}_{0.5})\text{NbO}_3-x\text{CaTiO}_3$ ¹³ solid solution systems. In addition, the Curie temperature T_c shifted linearly toward lower temperatures, as shown in Fig. 2(b). Therefore, these results also indicated that the sintered materials seemed to have formed a $\text{Li}_{0.06}(\text{Na}_{0.5}\text{K}_{0.5})_{0.94}\text{NbO}_3$ -based solid solution.

The microstructure of the $(1-x)\text{Li}_{0.06}(\text{Na}_{0.5}\text{K}_{0.5})_{0.94}\text{NbO}_3-x\text{BaTiO}_3$ ceramics with $0 \leq x \leq 0.07$ was investigated using SEM. Characteristic quasi-cubic grains could be observed for all the ceramics, as indicated in Fig. 3(a)–(e). The $\text{Li}_{0.06}(\text{Na}_{0.5}\text{K}_{0.5})_{0.94}\text{NbO}_3$ ceramic was composed of grains ranging 1.1–5.0 μm in size with the bimodal grain microstructure, as shown in Fig. 3(a). The apparent densities and average grain sizes of the sintered ceramics were shown in Fig. 4(a). As the content of Ba and Ti increased, the apparent density was increased and average grain size was decreased. Especially, the grain size distribution of $x=0.07$ specimen became narrow compared with that of the pure $\text{Li}_{0.06}(\text{Na}_{0.5}\text{K}_{0.5})_{0.94}\text{NbO}_3$ ceramics; the former microstructure was composed of grains ranging 0.5–2.2 μm in size. This result indicates that the improvement in the microstructure of $\text{Li}_{0.06}(\text{Na}_{0.5}\text{K}_{0.5})_{0.94}\text{NbO}_3$ ceramics could be performed by Ba and Ti substitution. Thereby, the frequency dispersion of dielectric constant for these samples was also reduced with increasing Ba and Ti content x , as indicated in Fig. 4(b).

In general, the sintering synthesis of alkaline niobate-based piezoelectric ceramics is performed at temperature near these melting points. As a result, abnormal grain growth tends to occur. On the other hand, adding some oxides with low melting points effectively can lower the sintering temperature and control their grain size to avoid abnormal grain growth.^{7–10} Small and uniform grain microstructure is

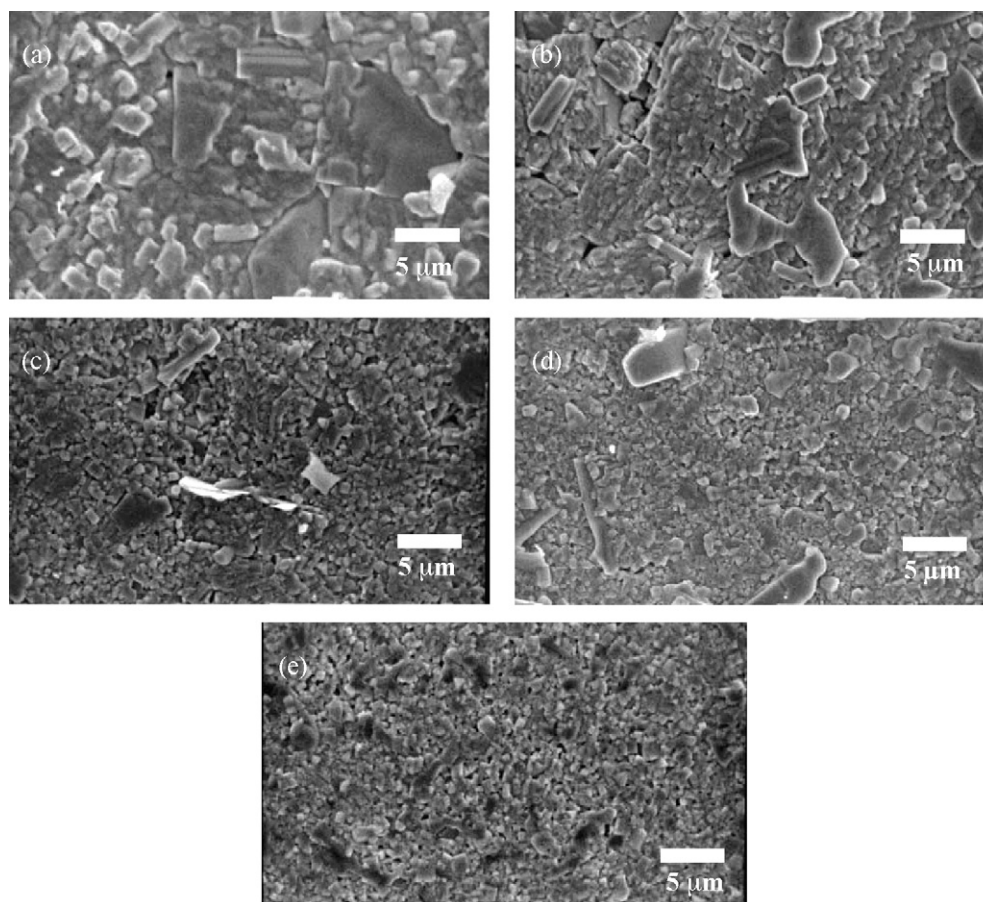


Fig. 3. SEM micrographs of $(1-x)\text{Li}_{0.06}(\text{Na}_{0.5}\text{K}_{0.5})_{0.94}\text{NbO}_3-x\text{BaTiO}_3$ sintered ceramics: (a) $x=0$, (b) $x=0.01$, (c) $x=0.03$, (d) $x=0.05$ and (e) $x=0.07$.

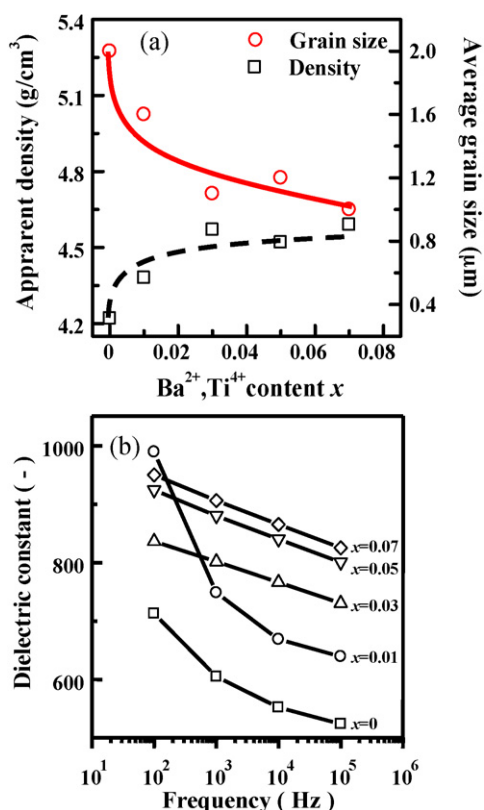


Fig. 4. (a) Grain size and density variations; (b) frequency dependence of dielectric constant of $(1-x)\text{Li}_{0.06}(\text{Na}_{0.5}\text{K}_{0.5})_{0.94}\text{NbO}_3-x\text{BaTiO}_3$ ($x=0-0.07$) ceramics.

required for piezoelectric ceramics showing a high mechanical strength to be applied in devices that yield mechanical force.^{6,14} In this study, TG-DTA measurement confirmed that the melting points of the $\text{Li}_{0.06}(\text{Na}_{0.5}\text{K}_{0.5})_{0.94}\text{NbO}_3$ ceramics ($x=0$) and $0.95\text{Li}_{0.06}(\text{Na}_{0.5}\text{K}_{0.5})_{0.94}\text{NbO}_3-0.05\text{BaTiO}_3$ ceramics ($x=0.05$) were around 1228 and 1245 °C, respectively, which indicates that both of Ba and Ti substitution rises the melting point of the $\text{Li}_{0.06}(\text{Na}_{0.5}\text{K}_{0.5})_{0.94}\text{NbO}_3$ ceramics. Based on this result, the sintering temperature of the ceramics was determined to be higher temperatures in proportion to x , as mentioned in Section 2. However, abnormal grain growth did not occurred even in samples with higher x , regardless of higher sintering temperature applied; but rather the grain size was decreased. In other words, abnormal grain growth was successfully inhibited and a fine microstructure could maintain as similar to the case where oxide additives with low melting points were utilized.

Fig. 5 shows the polarization–electric field (P – E) hysteresis loops of $(1-x)\text{Li}_{0.06}(\text{Na}_{0.5}\text{K}_{0.5})_{0.94}\text{NbO}_3-x\text{BaTiO}_3$ ceramics measured at 1 Hz. The piezoelectric properties of the sintered samples are also listed in Table 1. For all the specimens, typical P – E hysteresis loops were observed at room temperature. However, both $x=0$ and 0.01 samples could not show well-saturated hysteresis loops under a low electric field (40 kV/cm) because of the large leakage current and low resistivities as listed in Table 1. On the other hand, both $x=0.03$ and 0.05 samples demonstrated well-saturated hysteresis loops under a high electric field (100 kV/cm) because their resistivities were

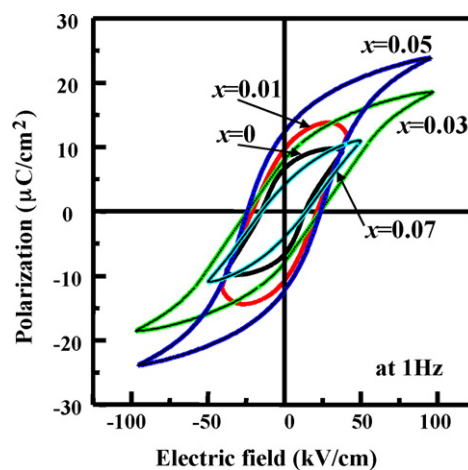


Fig. 5. Polarization–electric field (P – E) hysteresis loops of $(1-x)\text{Li}_{0.06}(\text{Na}_{0.5}\text{K}_{0.5})_{0.94}\text{NbO}_3-x\text{BaTiO}_3$ ($x=0-0.07$) ceramics measured at 1 Hz.

Table 1

Electric properties of $(1-x)\text{Li}_{0.06}(\text{Na}_{0.5}\text{K}_{0.5})_{0.94}\text{NbO}_3-x\text{BaTiO}_3$ ($x=0-0.07$) ceramics.

Composition x	d_{33} (pC/N)	k_p	Q_m	ρ (Ω cm)
0	209	0.33	44.3	5.03×10^{10}
0.01	100	0.26	19.9	9.13×10^9
0.03	128	0.32	91.8	1.42×10^{11}
0.05	101	0.27	120.8	8.33×10^{10}
0.07	64	0.17	128.4	4.16×10^{10}

1.42×10^{11} and $8.33 \times 10^{10} \Omega$ cm, which were higher than those of other compositions as listed in Table 1. Particularly, the remanent polarization (P_r) and coercive field (E_c) of $x=0.05$ ceramics indicated 12.7 $\mu\text{C}/\text{cm}^2$ and 23.4 kV/cm, respectively. Then, the piezoelectric constant (d_{33}) and the electromechanical coupling factor (k_p) of the Ba- and Ti-doped ceramics were lower than those of non-doped $\text{Li}_{0.06}(\text{Na}_{0.5}\text{K}_{0.5})_{0.94}\text{NbO}_3$ ceramics, due to the decrease of grain size. In fact, according to the relationship between d_{33} and the grain size of $\text{Pb}(\text{Zr}, \text{Ti})\text{O}_3$ -based ceramics,¹⁵ the d_{33} value decreases rapidly when the grain size is reduced. On the other hand, the mechanical quality factor (Q_m) of the sintered samples enhanced with increasing the Ba and Ti content. Especially, the Q_m of $x=0.07$ specimen reached 128.4, which was about three times higher than that of pure $\text{Li}_{0.06}(\text{Na}_{0.5}\text{K}_{0.5})_{0.94}\text{NbO}_3$ ceramics (44.3). This is due to both a decrease of grain size and uniform grain microstructure of the resultant ceramics, as shown in Figs. 3 and 4(a). As mentioned above, the piezoelectric ceramics usually require a homogeneous microstructure with a small grain size to enhance the mechanical strength of them. Therefore, it is considered that the grain size control for the piezoelectric ceramics plays important part to improve the mechanical quality factor Q_m .

4. Conclusion

Lead-free Ba- and Ti-doped $\text{Li}_{0.06}(\text{Na}_{0.5}\text{K}_{0.5})_{0.94}\text{NbO}_3$ ceramics were synthesized by using conventional solid state reaction method, and the microstructure and electric properties

of these samples were investigated. With increasing Ba and Ti content, the average grain size of these samples decreased from 2.0 to 0.9 μm , and the uniform microstructure was obtained. As a result, the frequency dispersion of dielectric constant for these samples was reduced and the mechanical quality factor Q_m of these samples was improved with increasing Ba and Ti content.

Acknowledgement

This work was financially supported by Industrial Technology Research Grant Program in 2007 from New Energy and Industrial Technology Development Organization (NEDO) of Japan.

References

- Guo, Y., Kakimoto, K. and Ohsato, H., Phase transitional behavior and piezoelectric properties of $(\text{Na}_{0.5}\text{K}_{0.5})\text{NbO}_3\text{--LiNbO}_3$ ceramics. *Appl. Phys. Lett.*, 2004, **85**, 4121–4123.
- Guo, Y., Kakimoto, K. and Ohsato, H., Structure and electrical properties of lead-free $(\text{Na}_{0.5}\text{K}_{0.5})\text{NbO}_3\text{--BaTiO}_3$ Ceramics. *Jpn. J. Appl. Phys.*, 2004, **43**, 6662–6666.
- Guo, Y., Kakimoto, K. and Ohsato, H., Dielectric and piezoelectric properties of lead-free $(\text{Na}_{0.5}\text{K}_{0.5})\text{NbO}_3\text{--SrTiO}_3$ ceramics. *Solid State Commun.*, 2004, **129**, 279–284.
- Saito, Y., Takao, H., Tani, T., Nonoyama, T., Takatori, K., Homma, T., Nagaya, T. and Nakamura, M., Lead-free piezoceramics nature. *Nature*, 2004, **432**, 84–87.
- Matsubara, M., Yamaguchi, T., Kikuta, K. and Hirano, S., Sintering and piezoelectric properties of potassium sodium niobate ceramics with newly developed sintering aid. *Jpn. J. Appl. Phys.*, 2005, **44**, 258–263.
- Matsubara, M., Kikuta, K. and Hirano, S., Piezoelectric properties of $(\text{K}_{0.5}\text{Na}_{0.5})(\text{Nb}_{1-x}\text{Ta}_x)\text{O}_3\text{--K}_{5.4}\text{CuTa}_{10}\text{O}_{29}$ ceramics. *J. Appl. Phys.*, 2005, **97**, 114105.
- Park, H., Choi, J., Choi, M., Cho, K., Nahm, S., Lee, H. and Kang, H., Effect of CuO on the sintering temperature and piezoelectric properties of $(\text{Na}_{0.5}\text{K}_{0.5})\text{NbO}_3$ lead-free piezoelectric ceramics. *J. Am. Ceram. Soc.*, 2008, **91**, 2374–2377.
- Park, H., Ahn, C., Cho, K., Nahm, S., Lee, H., Kang, H., Kim, D. and Park, K., Low-temperature sintering and piezoelectric properties of CuO-added $0.95(\text{Na}_{0.5}\text{K}_{0.5})\text{NbO}_3\text{--}0.05\text{BaTiO}_3$ ceramics. *J. Am. Ceram. Soc.*, 2007, **90**, 4066–4069.
- Park, S. H., Ahn, C. W., Nahm, S. and Song, J. S., Microstructure and piezoelectric properties of ZnO-added $(\text{Na}_{0.5}\text{K}_{0.5})\text{NbO}_3$ ceramics. *Jpn. J. Appl. Phys.*, 2004, **43**, L1072–L1074.
- Zuo, R., Rodel, J., Chen, R. and Li, L., Sintering and electrical properties of lead-free $\text{Na}_{0.5}\text{K}_{0.5}\text{NbO}_3$ piezoelectric ceramics. *J. Am. Ceram. Soc.*, 2006, **89**, 2010–2015.
- Ahn, C., Park, H., Nahm, S., Uchino, K., Lee, H. and Lee, H., Structural variation and piezoelectric properties of $0.95(\text{Na}_{0.5}\text{K}_{0.5})\text{NbO}_3\text{--}0.05\text{BaTiO}_3$ ceramics. *Sens. Actuators A*, 2007, **136**, 255–260.
- Cho, K., Park, H., Ahn, C., Nahm, S., Uchino, K., Park, S., Lee, H. and Lee, H., Microstructure and piezoelectric properties of $0.95(\text{Na}_{0.5}\text{K}_{0.5})\text{NbO}_3\text{--}0.05\text{SrTiO}_3$ ceramics. *J. Am. Ceram. Soc.*, 2007, **90**, 1946–1949.
- Park, H., Cho, K., Paik, D., Nahm, S., Lee, H. and Kim, D., Microstructure and piezoelectric properties of lead-free $(1-x)(\text{Na}_{0.5}\text{K}_{0.5})\text{NbO}_3\text{--}x\text{CaTiO}_3$ ceramics. *J. Appl. Phys.*, 2007, **102**, 124101.
- Chang, J. T. Y., Yang, Z. and Wei, L., Microstructure, density, and dielectric properties of lead-free $(\text{K}_{0.44}\text{Na}_{0.52}\text{Li}_{0.04})(\text{Nb}_{0.96-x}\text{Ta}_x\text{Sb}_{0.04})\text{O}_3$ piezoelectric ceramics. *J. Am. Ceram.*, 2007, **90**, 1656–1658.
- Takagi, K., Kikuchi, S., Li, J., Okumura, H., Watanabe, R. and Kawasaki, A., Ferroelectric and Photostrictive properties of fine-grained PLZT ceramics derived from mechanical alloying. *J. Am. Ceram. Soc.*, 2004, **87**, 1477–1482.